Neurobiology of Disease 121 (2019) 131–137

Contents lists available at ScienceDirect

Neurobiology of Disease

journal homepage: www.elsevier.com/locate/ynbdi

Single chain variable fragment antibodies directed against SOD1 ameliorate disease in mutant SOD1 transgenic mice

Ghanashyam D. Ghadge[a], Brian K. Kay[b], Claire Drigotas[a], Raymond P. Roos[a,*]

[a] Department of Neurology, University of Chicago Medical Center, 5841 S. Maryland Avenue, MC2030, Chicago, IL 60637, United States
[b] Department of Biological Sciences, University of Illinois at Chicago, 900 S. Ashland Ave., Molecular Biology Research Building, Room 4318, (M/C 567), Chicago, IL 60607, United States

ARTICLE INFO

Keywords:
Familial amyotrophic lateral sclerosis
Mutant superoxide dismutase type 1
Amyotrophic lateral sclerosis
ALS
Single chain fragments of variable region antibodies
scFvs
Motor neuron disease

ABSTRACT

Mutations in Cu/Zn superoxide dismutase (SOD1) are the cause of ~20% of cases of familial ALS (FALS), which comprise ~10% of the overall total number of cases of ALS. Mutant (mt) SOD1 is thought to cause FALS through a gain and not loss in function, perhaps as a result of the mutant protein's misfolding and aggregation. Previously we used a phage display library to raise single chain variable fragment antibodies (scFvs) against SOD1, which were found to decrease aggregation of mtSOD1 and toxicity in vitro. In the present study, we show that two scFvs directed against SOD1 ameliorate disease in G93A mtSOD1 transgenic mice and also decrease motor neuron loss, microgliosis, astrocytosis, as well as SOD1 burden and aggregation. The results suggest that the use of antibodies or antibody mimetics directed against SOD1 may be a useful therapeutic direction in mtSOD1-induced FALS. Since studies suggest that wild type SOD1 may be misfolded similar to that seen with mtSOD1, this therapeutic direction may be effective in sporadic as well as FALS.

1. Introduction

Amyotrophic lateral sclerosis (ALS) is a neurodegenerative disease characterized by the selective loss of motor neurons (motor neurons). Approximately 10% of ALS cases are familial (FALS), and ~20% of FALS cases are caused by mutations in Cu/Zn superoxide dismutase (SOD1)(reviewed in(Taylor et al., 2016)). Mutant (mt) SOD1-induced disease results from a gain-of-function rather than loss-of-function as evidenced by the following: some FALS-inducing mtSOD1s have full dismutase activity; mice that carry a mtSOD1 transgene develop ALS despite the mouse's normal endogenous SOD1 activity; deletion of SOD1 does not cause an ALS-like disease in mice. While the toxicity of mtSOD1 is not fully understood, misfolding and aggregation of mtSOD1 is a consistent feature of the pathology of mtSOD1-induced FALS in patients and mtSOD1 transgenic rodent models, and has been proposed to underlie the basis for motor neuron degeneration. Aggregates of mtSOD1 could cause toxicity by: sequestering SOD1-binding proteins that are critical to the viability of motor neurons; exposing a toxic domain of SOD1; or increasing ER stress and thereby overwhelming the unfolded protein response.

Misfolding with aggregation of specific disease-related proteins has been implicated in the pathogenesis of a number of neurodegenerative diseases. In some neurodegenerative diseases, antibodies have been used to disrupt misfolding of the cognate proteins, most notably in Alzheimer's disease, Parkinson's disease, and prion disease(Castillo-Carranza et al., 2014; Dematteos et al., 2012; Games et al., 2014; Roettger et al., 2013; Spencer et al., 2014 among other references).

In the case of ALS, initial studies from the Julien lab reported that: a) immunization with mtSOD1(Takeuchi et al., 2010; Urushitani et al., 2007) or a peptide within the SOD1 interface(Liu et al., 2012) delays disease onset and extends survival of FALS mtSOD1 transgenic mice; b) intraventricular infusion of anti-SOD1 monoclonal antibodies (mAbs) by an Alzet osmotic minipump into FALS transgenic mice significantly prolongs survival(Gros-Louis et al., 2010; Urushitani et al., 2007). These studies demonstrated that antibodies can be produced that are mtSOD1-specific and therapeutically effective in FALS. There are a number of possible mechanisms by which mtSOD1 antibodies could prolong survival of mtSOD1 transgenic mice: interference with aggregation, thereby preventing the sequestration of proteins that are important for motor neuron survival; masking a toxic domain of mtSOD1 that is exposed when SOD1 is misfolded; change in the conformation of misfolded mtSOD1, thereby attenuating the mutant's toxicity and down-regulating expression of mtSOD1.

We previously used phage display to generate anti-SOD1 single

* Corresponding author at: Department of Neurology/MC2030, University of Chicago Medical Center, 5841 S. Maryland Ave., Chicago, IL 60637, United States
E-mail addresses: gghadge@neurology.bsd.uchicago.edu (G.D. Ghadge), bkay@uic.edu (B.K. Kay), drigotasc@uchicago.edu (C. Drigotas), rroos@neurology.bsd.uchicago.edu (R.P. Roos).

https://doi.org/10.1016/j.nbd.2018.08.021
Received 2 April 2018; Received in revised form 13 August 2018; Accepted 30 August 2018
Available online 31 August 2018
0969-9961/

chain variable fragment antibodies (scFvs) (Ghadge et al., 2013), which have the variable domains of the immunoglobulin IgG heavy (V_H) and light (V_L) chains joined by a linker peptide sequence. scFvs have several advantages over mAbs: they can be readily cloned, expressed intracellularly, and used in gene delivery studies. The small size of scFvs makes them amenable to intracellular delivery and activity as "intrabodies." For these reasons, scFvs have been produced against misfolded proteins that are associated with a number of neurodegenerative diseases. Two of the anti-SOD1 scFvs that we originally described decreased mtSOD1 aggregation and mtSOD1-induced cell death in vitro. The present study characterizes the effect of these scFvs delivered by an adeno-associated virus 9 vector (AAV) on disease of mtSOD1 transgenic mice.

2. Materials and methods

2.1. Mice and breeding

Animal experiments were performed in compliance with the NIH Guide for the Care and Use of Laboratory Animals, and the approval of the University of Chicago Institutional Animal Care and Use Committee. G93ASOD1 transgenic mice on a C57BL/6 J background (Wooley et al., 2005) from Jackson Labs (Bar Harbor, ME; strain 004435) were bred and genotyped by PCR using the following primers for the detection of SOD1 (Forward, 5′-CATCAGCCCTAATCCATCTGA-3′; Reverse, 5′-CGC GACTAACAATCAAAGTGA-3′) gene. Both male and female mice were used for the studies since no difference in their clinical phenotype was found in a previous investigation(Wooley et al., 2005).

2.2. scFvs and adeno-associated virus vector (AAV)

We inserted scFvB1 and scFvB12 that contained a FLAG tag at the N-terminus between the *Eco*RI and *Xho*I restriction sites of the shuttle vector pENN.AAV.CB7.CI.rBG using primers (forward 5′-CCGGAATTC ACCATGGACTACAAGGACGACGATGAC-3′ and reverse 5′-CCGCTCGA GTCACAGATCCTCTTCTGAGATGAGTTTTTGTTCGTCGACTGAGGAGA CGGTGACC-3′) for AAV9 vector production. AAV:scFvB1 and AAV:scFvB12 were subsequently prepared by the Virus Vector Core of the University of Pennsylvania. We also received AAV-GFP (AAV9.CB7.CI.eGFP.WPRE.rBG) virus vector as a control. G93ASOD1 transgenic mice were injected with 5×10^{11} virus genome copies in the facial vein as neonates (P1) or in the tail vein when ~120-day-old.

2.3. Assessment of disease phenotype

Clinical assessment. Mice were weighed every two days and clinically assessed as previously described (Boillee et al., 2006): onset of disease was defined as peak weight before a decline; early phase of disease was the period from peak weight until loss of 10% of maximal weight; late phase of disease was the time from 10% loss in weight until death (when a mouse was unable to right itself within 20 s after being put on its back). In experiments monitoring disease parameters and survival, the AAV:scFvB1- and AAV:scFvB12-treated mice were compared with mice treated with AAV:GFP as well as littermate untreated G93ASOD1 mice. Nontransgenic littermate mice were used as additional controls in experiments.

2.4. Pathology and immunohistochemical evaluation

Mice at age of ~155 days were compared with respect to spinal cord motor neuron count, SOD1 burden and aggregation, microgliosis, and astrocytosis as previously described (Wang et al., 2014). Mice were anesthetized and perfused transcardially using cold phosphate buffered saline (PBS) followed by 4% paraformaldehyde and post-fixed overnight. The expression of the scFv was assessed in the spinal cord by immunofluorescent staining using anti-Flag antibody (1:100 dilution, Cell Signaling Technology, Danvers, MA) followed by Alexa Fluor 594 anti-rabbit secondary antibody (1:500 dilution, Invitrogen). Four to 12 sections of the anterior horn of the cervical and lumbar spinal cord from each of at least 3 G93ASOD1 mice were processed for Nissl staining to assess motor neuron numbers, and processed for immunofluorescent staining to detect SOD1 burden and aggregation. SOD1 aggregates were identified as puncta of dense fluorescent staining by using a rabbit antibody that recognizes the carboxyl end of mouse and human SOD1 [1:3000 dilution,(Deng et al., 2006)] followed by Alexa Fluor 594 goat anti-rabbit secondary antibody (1:1000 dilution, Invitrogen), as previously described (Wang et al., 2014). SOD1 burden was measured as the percent anti-SOD1 positive area in the sections using ImageJ software. Reactive microglia and astrocytes were detected by using rabbit anti-IbaI (ionized calcium-binding adaptor molecule 1 (1:1000 dilution, Wako, Richmond, VA) and mouse anti-GFAP (glial fibrillary acid protein) (1:1000 dilution, Chemicon, Temecula, CA) primary antibodies respectively followed by either anti-rabbit HRP or anti-mouse HRP (ImmPRESS Reagents, Vector Labs, Burlingame, CA) according to the manufacturer's instructions. Nissl-stained sections of the spinal cord were blinded, and motor neurons (characterized as cells larger than 18.5 μM in size) were counted using ImageJ software. Motor neurons were also assessed by choline acetyl transferase (ChAT) staining using rabbit anti-ChAT antibody (1:100 dilution, Chemicon, Temecula, CA) followed by anti-rabbit Alexa Fluor 488 secondary antibody (1:500 dilution, Invitrogen).

2.5. Statistics

The data were statistically analyzed by *t*-test or one-way ANOVA using GraphPad Prism 7 software.

3. Results

3.1. scFvB1 and scFvB12 ameliorate disease in G93ASOD1 transgenic mice

We previously generated two anti-SOD1 scFvs, B1 and B12, that decrease mtSOD1 aggregation and mtSOD1-induced cell death in vitro (Ghadge et al., 2013). In order to test their effect on G93ASOD1 mice, we prepared AAV9 vectors that encode the scFvs. We injected the AAVs intravenously (IV) into G93ASOD1 neonatal mice (which delivers the transgene primarily to neurons, including ~60% lumbar spinal cord motor neurons) or adults (which delivers the transgene primarily to glial cells)(Foust et al., 2009). The adult mice were injected at ~120 days, just before the onset of disease, which was defined as the peak weight prior to the decline of weight that occurs during disease. A group of uninjected G93SOD1 mice had an onset of disease of 130 ± 2.3 days, and a mean survival of 156 ± 2.5 days. Of note, there was no clinical abnormality or significant neuropathology in a non-transgenic mouse that received AAV:scFvB1 neonatally and was sacrificed at age of 5 months.

There was no significant difference in the onset of disease in AAV:scFvB1-injected neonatal G93ASOD1 mice ($n = 24$) compared to control AAV:GFP-injected neonatal G93ASOD1 mice($n = 10$): 123 ± 1.4 days vs. 122 ± 1.6 days respectively ($P > .05$) (Fig. 1A). Despite the similar onset of disease, the neonatal G93ASOD1 mice injected with AAV:scFvB1 survived for 174 ± 1.5 days compared with control AAV:GFP-injected mice, which survived for a mean of 147 ± 4.4 days ($P < .0001$) (Fig. 1A). The increase in survival in scFvB1-injected G93ASOD1 mice was similar in both males and females ($P > .05$, data not shown). The prolongation in survival was related to a longer duration in both the early and late phases of disease. The early phase of disease of AAV:scFvB1-injected neonate mice lasted 30 ± 2.1 days compared to 18 ± 2.9 days found with AAV:GFP-injected neonates ($P < .01$) (Fig. 1B). The late phase of disease of AAV:scFvB1-injected mice lasted 22 ± 1.7 days compared to 6 ± 2.2 days in AAV:GFP-injected neonates ($P < .0001$) (Fig. 1C).

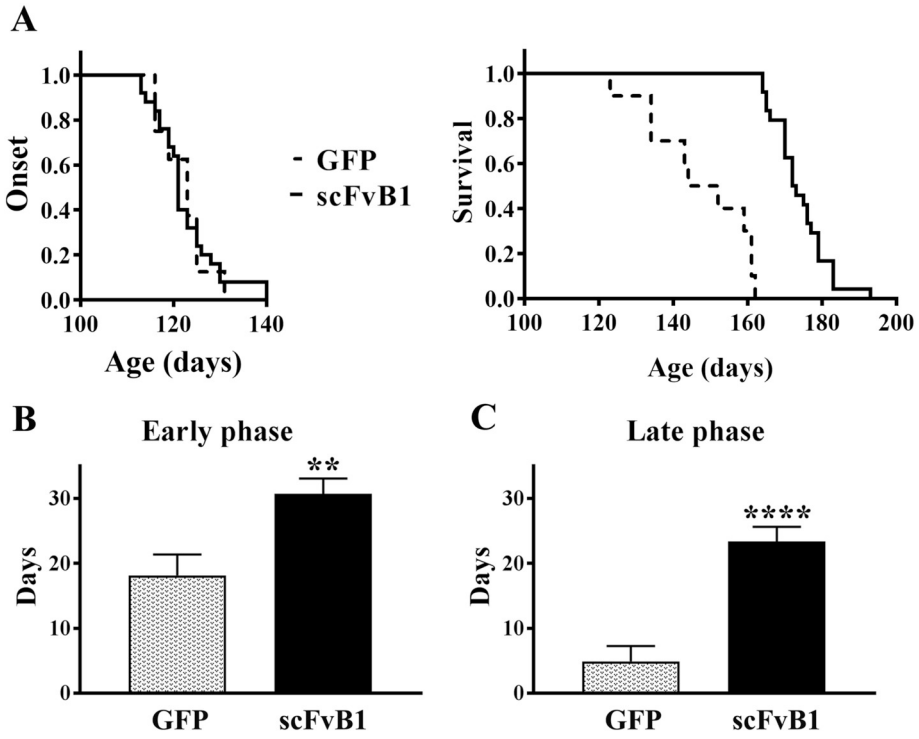

Fig. 1. Amelioration of disease following IV injection of neonatal G93ASOD1 mice with AAV:scFvB1 and AAV:GFP. Plots of (A) disease onset and survival, and bar diagrams with standard error of the mean of (B) the early phase of disease, and (C) late phase. The onset of the disease was similar in the scFvB1-treated and control groups; however, AAV:scFvB1-injected mice survived longer than the control AAV:GFP –injected mice due to prolongation of the early as well as late disease phase. In the Y axis of A, 1 refers to the total number of animals. ** = $P < .01$, **** = $P < .0001$.

Neonatal injection of AAV:scFvB12 could not be assessed because the inoculum was toxic.

There was no significant difference in the onset of disease in AAV:scFvB1-injected ($n = 13$) and AAV:scFvB12-injected ($n = 11$) adult G93ASOD1 mice compared to control AAV:GFP-injected adult G93ASOD1 mice (n = 13): 128 ± 2.2 and 128 ± 2.3 days vs. 130 ± 1.8 days respectively ($P > .05$) (Fig. 2A). However, adult G93ASOD1 mice injected with AAV:scFvB1 and AAV:scFvB12 survived for 175 ± 2.5 and 172 ± 2.3 days respectively (Fig. 2A), which was significantly longer than the ~161 day survival found with AAV:GFP-injected mice: AAV:scFvB1 vs. AAV:GFP, $P < .001$; AAV:scFvB12 vs. AAV:GFP, $P < .05$. The prolongation in survival was not related to a delay in the onset of disease (which followed relatively soon after the injection), but was a result of an increased duration of the late phase of disease. The early phase of disease of both AAV:scFvB1-injected and AAV:scFvB12-injected adult mice lasted 28 ± 2.6 and 28 ± 2.9 days respectively compared to 23 ± 2.4 days found with AAV:GFP-injected adults ($P > .05$) (Fig. 2B). In contrast, the late phase of disease in AAV:scFvB1-injected adult mice(19 ± 1.8 days) and in AAV:scFvB12-injected adult mice (15 ± 2.1 days) was significantly longer than in

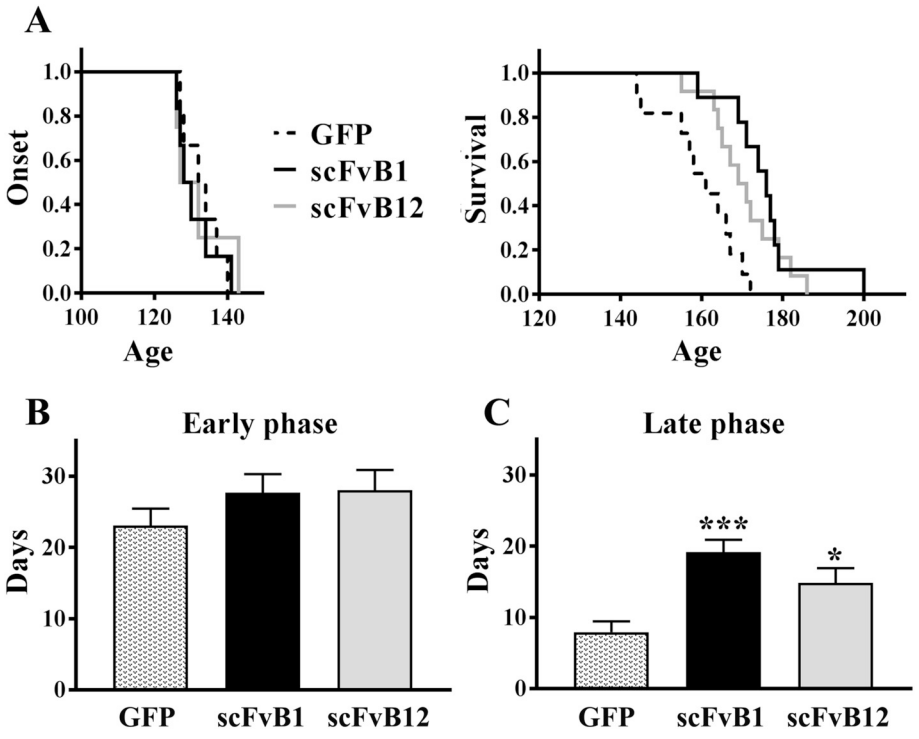

Fig. 2. Amelioration of disease following IV injection of adult G93ASOD1 mice with AAV:scFvB1, AAV:scFvB12, and AAV:GFP. Plots of (A) disease onset and survival as well as bar diagrams with standard error of the mean of (B) the early phase of disease and (C) late phase of disease. The onset of disease was similar in the scFv-treated and control groups; however, AAV:scFvB1- and AAV:scFvB12-injected mice survived longer than control AAV:GFP-injected mice due to prolongation of the late phase of the disease. In the Y axis of A, 1 refers to the total number of animals.* = $P < .05$, *** = $P < .001$.

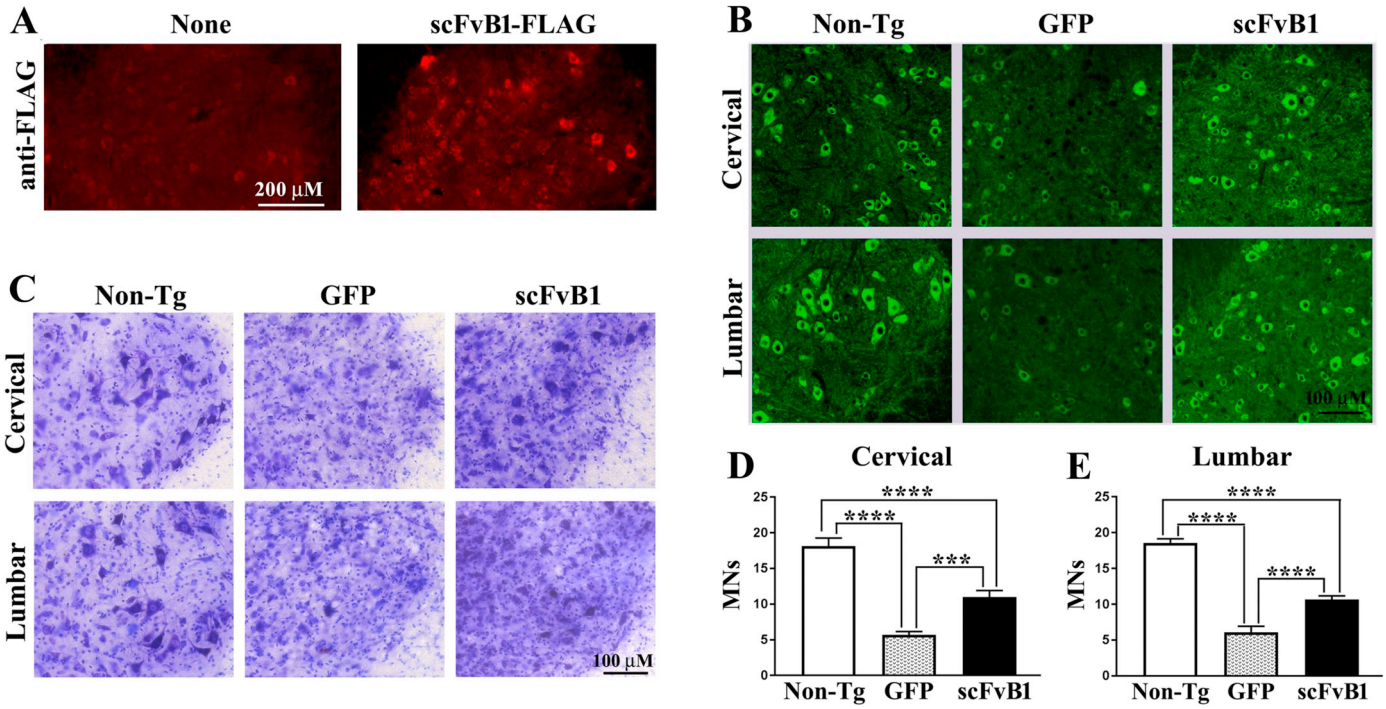

Fig. 3. Increased motor neuron survival in neonatal G93ASOD1 mice injected with AAV:scFvB1. (A) scFvB1 is expressed in motor neurons 110 days after IV injection of AAV:scFvB1 into neonatal mice. Representative ChAT (B) and Nissl-stained (C) sections of the cervical and lumbar spinal cord, and bar diagrams with standard error of the mean showing the number of Nissl-stained motor neurons in hemisections of the anterior horn of the cervical (D) and lumbar (E) spinal cord from non-transgenic (non-Tg), AAV:GFP-injected, and AAV:scFvB1-injected mice. AAV:scFvB1-injected G93ASOD1 mice showed a significantly higher number of motor neurons in cervical and lumbar sections of the spinal cord than present in AAV:GFP-injected mice.*** = $P < .001$, **** = $P < .0001$.

AAV:GFP-injected adult mice (8 ± 1.5 days) ($P < .001$ and $P < .05$ respectively) (Fig. 2C).

3.2. AAV:scFvB1- and AAV:scFvB12-injected G93ASOD1 transgenic mice have less motor neuron loss and fewer SOD1 aggregates than AAV:GFP-injected G93ASOD1 mice

In order to compare features of the pathology of AAV:scFvB1- and AAV:scFvB12-treated with AAV:GFP-treated G93ASOD1 mice, we examined the number of motor neurons and SOD1 aggregates in treated mice at end stage. There was a similar loss of motor neurons and number of SOD1 aggregates at end stage in the AAV:scFvB1-, AAV:scFvB12-, and AAV-GFP-injected G93ASOD1 mice (data not shown). For this reason, we compared the number of motor neurons and SOD1 burden and aggregation in AAV:scFvB1-injected neonatal mice at ~155 days of age with similarly aged AAV:GFP-injected mice.

We first tested whether the target cell expressed the transgene following the AAV neonatal injection. Expression of scFvB1 was detected in motor neurons at day 110 following IV AAV:scFvB1 injection of neonatal mice (Fig. 3A). Following neonatal mouse injection, there was significant motor neuron loss in cervical and lumbar spinal cords of AAV:GFP and AAV:scFvB1-injected G93ASOD1 mice when compared to nontransgenic mice ($P < .0001$); however, AAV:scFvB1-injected G93ASOD1 neonatal mice had significantly less motor neuron loss in both the anterior horn of the cervical and lumbar spinal cord than was present in AAV:GFP-injected G93ASOD1 mice ($P < .001$ and $P < .0001$ respectively) (Fig. 3B-E).

Anti-SOD1 staining was decreased in the anterior horn of the cervical and lumbar spinal cords of G93ASOD1 mice treated with scFvB1 as a neonate compared to GFP-treated mice ($P < .01$ and $P < .0001$ respectively) (Fig. 4). Compared to AAV:GFP-injected neonatal mtSOD1 mice, AAV:scFvB1-injected mice had a decreased burden of SOD1 as reflected by the overall decrease in SOD1 immunoflourescence in cervical and lumbar spinal cord sections (Fig. 4B). Abundant small SOD1 aggregates were present in spinal cord sections stained with anti-SOD1 antibody from AAV:scFvB1 and AAV:GFP-injected mtSOD1 mice; however, there were significantly fewer aggregates in the anterior horn of the cervical and lumbar spinal cords of G93ASOD1 mice injected with the AAV:scFvB1 compared to mice injected with AAV:GFP ($P < .05$ and $P < .001$ respectively)(Fig. 4A, C).

3.3. AAV:scFvB1-injected G93ASOD1 mice exhibited less microgliosis and astrogliosis than AAV:GFP-injected G93ASOD1 mice

Microgliosis and astrocytosis are key pathological features of mutant SOD1 transgenic mice. We investigated these findings in mice at ~155 days of age, which is usually around the end stage of disease for G93ASOD1 transgenic mice. Sections from cervical and lumbar spinal cords of G93ASOD1 mice that had been neonatally injected with AAV:GFP or AAV:scFvB1 or were not treated were stained for Iba1 and GFAP positive cells. Importantly, AAV:scFvB1-treated G93ASOD1 mice showed a significant reduction in reactive microglia ($p < .0001$) as well as GFAP-positive astrocytes ($p < .05$) compared to AAV:GFP-injected mice (Fig. 5 A, B and C). In addition, reactive microglia and astrocytosis were increased in AAV:GFP injected G93ASOD1 mice as compared to nontransgenic mice (Fig. 5A). There was minimal if any microgliosis and astrocytosis in nontransgenic mice that received AAV:scFvB1 neonatally when sacrificed at age of 5 months.

4. Discussion

mtSOD1 is the cause of ~20% of FALS, and FALS comprises ~10% of the total cases of ALS. mtSOD1 is thought to be pathogenic because of a toxicity, that is thought to be related to its misfolding, rather than a loss in function(reviewed in(Taylor et al., 2016)). Antibodies prepared against misfolded proteins that accumulate in neurodegenerative disease have been shown to reduce their toxicity(Huang et al., 2013). As a result, multiple efforts are underway to develop and test

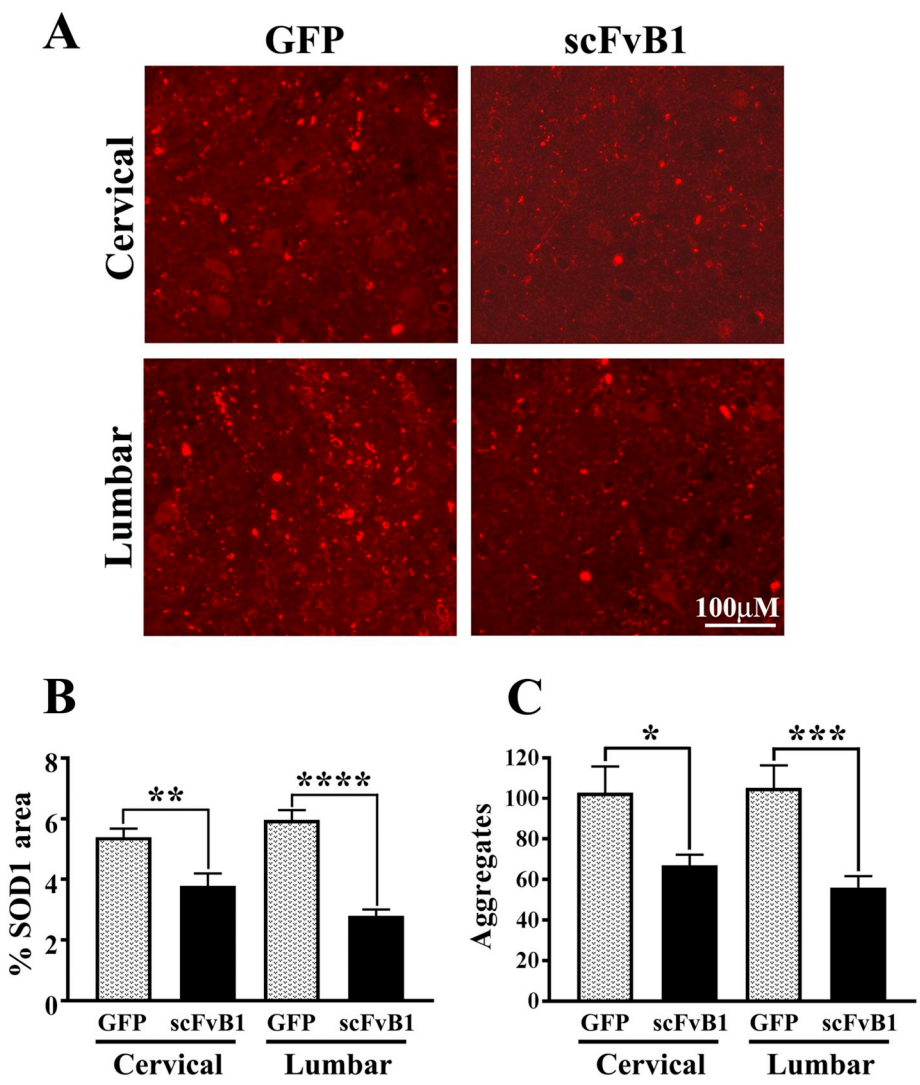

Fig. 4. Decreased SOD1 burden and aggregation following AAV:scFvB1 injection of neonatal G93ASOD1 mice. Representative sections of the anterior horn region of the cervical and lumbar spinal cord (A) stained with anti-SOD1 antibody, and bar diagrams with standard error of the mean showing percent anti-SOD1 positive area (B) and the number of aggregates (C) in hemisections of the anterior horn of the cervical and lumbar spinal cord from AAV:GFP-injected and AAV:scFvB1-injected mice. SOD1 burden and the number of SOD1 aggregates was significantly reduced in the anterior horn of cervical and lumbar regions of the spinal cord of G93ASOD1 mice injected with AAV:scFvB1 compared to the AAV:GFP-injected mice.* = $P < .05$, ** = $P < .01$, *** = $P < .001$ and **** = $P < .0001$.

immunotherapeutic regimens, e.g., Aducanumab(Sevigny et al., 2016), which targets extracellular amyloid-β in Alzheimer's disease, is currently in phase 3 clinical trials. These antibodies are presumed to act by inhibiting neuronal uptake and cell-to-cell propagation of misfolded protein species, and by removing extracellular aggregates via microglial opsonization of antibody-aggregate complexes. In some cases, investigators have prepared scFvs, presumably because of their advantages over conventional antibodies, such as their capacity to be delivered intracellularly as intrabodies.

A number of investigations have been mounted to test the effect of anti-SOD1 antibody in mtSOD1 transgenic mice. These studies have included active immunization with mtSOD1 and with an SOD1 peptide as well as intraventricular delivery of an anti-SOD1 mAb(Gros-Louis et al., 2010; Liu et al., 2012; Takeuchi et al., 2010; Urushitani et al., 2007). Furthermore, the Julien lab prepared a scFv from anti-SOD1 mAb with a murine immunoglobulin–secretory signal(Patel et al., 2014). The scFv was encoded in an AAV serotype-2/1 vector and delivered to 45-day-old G93ASOD1 mice by a single intrathecal injection. Following this treatment, mice survived for 159 days compared to 143 days survival following injection with a control AAV. There was evidence of a delay in motor neuron loss, axonal degeneration, microgliosis, astrocytosis, and misfolded SOD1 in the mice. The survival benefit of these mice was related to a delay in onset and not an extension of the clinical disease.

We previously generated anti-SOD1 scFvs by means of phage display, and showed that two of the scFvs, B1 and B12, decreased SOD1 aggregation and toxicity in vitro(Ghadge Ghadge et al., 2013). The present study investigated the effect on disease and pathology of G93A mice following IV injection of these two scFvs encoded by AAV9 when delivered into neonatal and adult G93ASOD1 mice. We were unable to test AAV:scFvB12 when delivered into neonatal mice because of toxicity; however, both AAV:scFvB1 and AAV:scFvB12 injection of adult mice significantly prolonged survival. The longest survival benefit was seen with AAV:scFvB1 injection into neonatal mice, presumably because there was an earlier and more prolonged duration for the scFv to act than following the adult injection. Also of importance is the observation that AAV IV injection of neonates leads to delivery of the transgene primarily into motor neurons, a key cell that undergoes dysfunction and death in ALS, while IV injection of adult mice leads to delivery primarily into glial cells(Foust et al., 2009). It is noteworthy that AAV:scFvB1 and AAV:scFvB12 injections of adult G93ASOD1 mice had a significant prolongation in survival despite the targeting into glia following an IV injection. The effect of adult injections probably reflects the importance of non-cell autonomous neurodegeneration in mtSOD1-induced ALS mice(Ilieva et al., 2009; Wang et al., 2011; Wang et al., 2012; Wang et al., 2008; Wang et al., 2009; Zhang et al., 2007), and the recognition that oligodendrocyte and astrocytic expression of mtSOD1 has a very significant effect on disease(Kang et al., 2013).

The main reason for the prolongation of survival following delivery of the scFvs was an effect on duration of disease. Experiments by Foust

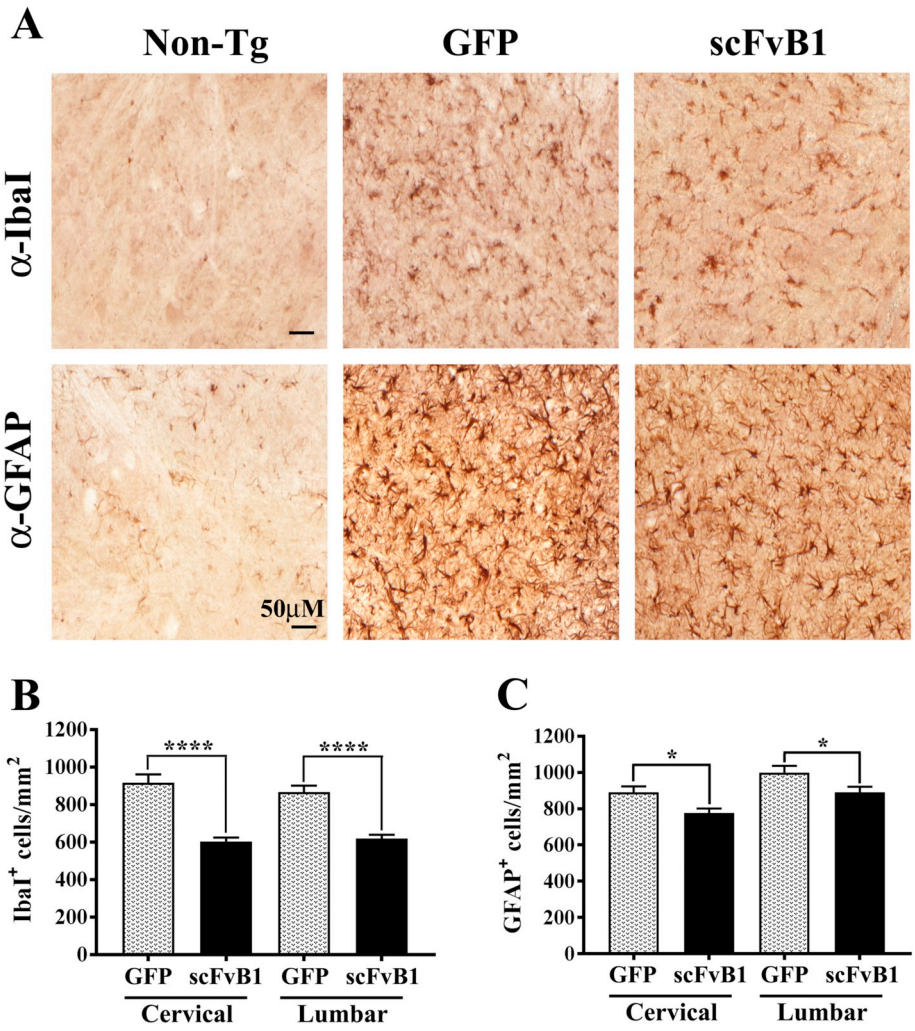

Fig. 5. Microgliosis and astrogliosis are decreased in neonatal G93ASOD1 mice injected with AAV:scFvB1. (A) Representative sections of immunohistochemical staining with IbaI and GFAP antibodies of the lumbar spinal cord of nontransgenic mice (left panels), AAV:GFP-injected G93ASOD1 mice (middle panels) and AAV:scFvB1-injected G93ASOD1 mice (right panels). (B) and (C) show bar diagrams with standard error of the mean indicating the number of reactive microglia (Iba1 + cells) and astrocytes (GFAP + cells) in sections of the cervical and lumbar spinal cord of AAV:GFP-injected and AAV:scFvB1-injected G93ASOD1 mice. Microgliosis and astrocytosis were reduced in G93ASOD1 mice injected with AAV:scFvB1 when compared to AAV:GFP-injected mice. Nontransgenic mice had little if any evidence of reactive microglia and astrocytes. * = $P < .05$ and **** = $P < .0001$.

et al.(Foust et al., 2013) similarly found that the prolongation in survival following IV injection of AAV9-mediated delivery of siRNA against mtSOD1 into 85 day old G93ASOD1 mice was a result of an effect on disease duration. In contrast, the Julien lab found that an anti-SOD1 scFv affected the onset rather than duration of disease. This difference may be a result of the different epitopes of the scFv, the different delivery routes, and the timing of the injections.

AAV:scFvB1-injected mice sacrificed at ~155 days showed a relative preservation of motor neurons and less aggregation of SOD1, microgliosis and astrocytosis when compared with AAV:GFP-injected mice. We suspect that this delay in pathology compared to control-treated mice was the reason for the prolongation in survival of AAV:scFvB1-treated mice.

In summary, we found that anti-SOD1 scFvs encoded in AAV9 and delivered to neonatal and 120 day old G93ASOD1 mice had a significant amelioration in disease, with a delay in duration and prolonged survival compared to control-treated mice. There was a corresponding delay in pathology in the spinal cords of anti-SOD1 scFv-treated mice. These results suggest that the use of antibodies directed against SOD1 may be a useful therapeutic direction in mtSOD1-induced FALS, presumably because interventions that decrease the amount of misfolded SOD1 can be an effective treatment. This therapeutic direction may be enhanced with the use of antibody mimetics, such as designed ankyrin repeat proteins (DARPins)(Jost and Pluckthun, 2014), which do not have many of the limitations of antibodies. Although studies are ongoing examining other ways of knocking down the expression of SOD1, such as through administration of anti-sense oligonucleotides that target SOD1(Miller et al., 2013), it is likely that multiple varied therapies will be needed in the treatment of ALS.

Acknowledgments

This work was supported by a grant from the ALS Association (RPR), the Pape Adams Charitable Foundation (RPR), and the Chicago Biomedical Consortium with support from the Chicago Community Trust (RPR, BK). We acknowledge the technical assistance of Qianyi (Lucy) Huang for some of these studies.

References

Boillee, S., et al., 2006. Onset and progression in inherited ALS determined by motor neurons and microglia. Science 312, 1389–1392.

Castillo-Carranza, D.L., et al., 2014. Passive immunization with Tau oligomer monoclonal antibody reverses tauopathy phenotypes without affecting hyperphosphorylated neurofibrillary tangles. J. Neurosci. 34, 4260–4272. https://doi.org/10.1523/JNEUROSCI.3192-13.2014.

Demattos, R.B., et al., 2012. A plaque-specific antibody clears existing beta-amyloid plaques in Alzheimer's disease mice. Neuron 76, 908–920. https://doi.org/10.1016/j.neuron.2012.10.029.

Deng, H.X., et al., 2006. Conversion to the amyotrophic lateral sclerosis phenotype is associated with intermolecular linked insoluble aggregates of SOD1 in mitochondria. Proc. Natl. Acad. Sci. U. S. A. 103, 7142–7147 (Epub 2006 Apr 24).

Foust, K.D., et al., 2009. Intravascular AAV9 preferentially targets neonatal neurons and adult astrocytes. Nat. Biotechnol. 27, 59–65 (Epub 2008 Dec 21).

Foust, K.D., et al., 2013. Therapeutic AAV9-mediated suppression of mutant SOD1 slows

disease progression and extends survival in models of inherited ALS. Mol. Ther. 21, 2148–2159.
Games, D., et al., 2014. Reducing C-terminal-truncated alpha-synuclein by immunotherapy attenuates neurodegeneration and propagation in Parkinson's disease-like models. J. Neurosci. 34, 9441–9454. https://doi.org/10.1523/JNEUROSCI.5314-13.2014.
Ghadge, G.D., et al., 2013. Single chain variable fragment antibodies block aggregation and toxicity induced by familial ALS-linked mutant forms of SOD1. Neurobiol. Dis. 56, 74–78. https://doi.org/10.1016/j.nbd.2013.04.007. (Epub 2013 Apr 20).
Gros-Louis, F., et al., 2010. Intracerebroventricular infusion of monoclonal antibody or its derived Fab fragment against misfolded forms of SOD1 mutant delays mortality in a mouse model of ALS. J. Neurochem. 113, 1188–1199.
Huang, L., et al., 2013. Single-chain fragment variable passive immunotherapies for neurodegenerative diseases. Int. J. Mol. Sci. 14, 19109–19127.
Ilieva, H., et al., 2009. Non-cell autonomous toxicity in neurodegenerative disorders: ALS and beyond. J. Cell Biol. 187, 761–772 (Epub).
Jost, C., Pluckthun, A., 2014. Engineered proteins with desired specificity: DARPins, other alternative scaffolds and bispecific IgGs. Curr. Opin. Struct. Biol. 27, 102–112. https://doi.org/10.1016/j.sbi.2014.05.011. (Epub 2014 Jul 15).
Kang, S.H., et al., 2013. Degeneration and impaired regeneration of gray matter oligodendrocytes in amyotrophic lateral sclerosis. Nat. Neurosci. 16, 571–579.
Liu, H.N., et al., 2012. Targeting of monomer/misfolded SOD1 as a therapeutic strategy for amyotrophic lateral sclerosis. J. Neurosci. 32, 8791–8799.
Miller, T.M., et al., 2013. An antisense oligonucleotide against SOD1 delivered intrathecally for patients with SOD1 familial amyotrophic lateral sclerosis: a phase 1, randomised, first-in-man study. Lancet Neurol. 12, 435–442.
Patel, P., et al., 2014. Adeno-associated virus-mediated delivery of a recombinant single-chain antibody against misfolded superoxide dismutase for treatment of amyotrophic lateral sclerosis. Mol. Ther. 22, 498–510. https://doi.org/10.1038/mt.2013.239. (Epub 2013 Oct 17).
Roettger, Y., et al., 2013. Immunotherapy in prion disease. Nat. Rev. Neurol. 9, 98–105.
Sevigny, J., et al., 2016. The antibody aducanumab reduces Aβ plaques in Alzheimer's disease. Nature 537, 50–56.
Spencer, B., et al., 2014. ESCRT-mediated uptake and degradation of brain-targeted alpha-synuclein single chain antibody attenuates neuronal degeneration in Vivo. Mol. Ther. 22, 1753–1767.
Takeuchi, S., et al., 2010. Induction of protective immunity by vaccination with wild-type apo superoxide dismutase 1 in mutant SOD1 transgenic mice. J. Neuropathol. Exp. Neurol. 69, 1044–1056.
Taylor, J.P., et al., 2016. Decoding ALS: from genes to mechanism. Nature 539, 197–206. https://doi.org/10.1038/nature20413.
Urushitani, M., et al., 2007. Therapeutic effects of immunization with mutant superoxide dismutase in mice models of amyotrophic lateral sclerosis. Proc. Natl. Acad. Sci. U. S. A. 104, 2495–2500.
Wang, L., et al., 2008. Restricted expression of mutant SOD1 in spinal motor neurons and interneurons induces motor neuron pathology. Neurobiol. Dis. 29, 400–408 (Epub 2007 Oct 23).
Wang, L., et al., 2009. The effect of mutant SOD1 dismutase activity on non-cell autonomous degeneration in familial amyotrophic lateral sclerosis. Neurobiol. Dis. 35, 234–240 (Epub 2009 May 12).
Wang, L., et al., 2011. Astrocyte loss of mutant SOD1 delays ALS disease onset and progression in G85R transgenic mice. Hum. Mol. Genet. 20, 286–293.
Wang, L., et al., 2012. Selective knockdown of mutant SOD1 in Schwann cells ameliorates disease in G85R mutant SOD1 transgenic mice. Neurobiol. Dis. 48, 52–57.
Wang, L., et al., 2014. An enhanced integrated stress response ameliorates mutant SOD1-induced ALS. Hum. Mol. Genet. 23, 2629–2638.
Wooley, C.M., et al., 2005. Gait analysis detects early changes in transgenic SOD1(G93A) mice. Muscle Nerve 32, 43–50.
Zhang, F., et al., 2007. Interaction between familial amyotrophic lateral sclerosis (ALS)-linked SOD1 mutants and the dynein complex. J. Biol. Chem. 282, 16691–16699 (Epub 2007 Apr 2).